ELSEVIER

Contents lists available at ScienceDirect

Biofilm

journal homepage: www.sciencedirect.com/journal/biofilm



Legionella affects biofilm structural response to detachment upon shear stress increase

Ana Rosa Silva ^a, C. William Keevil ^b, Ana Pereira ^{a,*}

- a LEPABE, ALICE, Faculty of Engineering, University of Porto, Rua Dr. Roberto Frias, 4200-465 Porto, Portugal
- ^b School of Biological Sciences, University of Southampton, Southampton, United Kingdom

ARTICLE INFO

Keywords:
Biofilm removal
Hydraulic management
Legionella control
Legionella spatial positioning
VBNC state
Water systems

ABSTRACT

Poor hydraulic management at water systems is associated with an increased risk of Legionnaires' disease caused by Legionella. Stagnation periods, followed by sudden water flow, can promote biofilm detachment and the release of Legionella into the bulk water. Regardless of its importance, the simultaneous effects of shear stress on biofilm detachment and Legionella release into the bulk water remain poorly understood. This study investigates how shear stress affects biofilms containing Legionella pneumophila in terms of: a) biofilm detachment, b) release of L. pneumophila into the bulk phase, and c) shifting of L. pneumophila into the viable but nonculturable (VBNC) state. Pseudomonas fluorescens biofilms were formed in a Center for Disease Control (CDC) biofilm reactor at 125 RPM and spiked with L. pneumophila. After 6 days, the system was set for 48 h to stagnation before flow was resumed at rotational velocities of 125, 225, and 400 RPM, corresponding to turbulent regimes with Reynolds numbers of 1552, 2794 and 4966, respectively. Biofilm properties, L. pneumophila viability, culturability, and spatial distribution were monitored. Results show that biofilms containing L. pneumophila maintained a similar basal thickness (12 µm) despite the detachment of the upper layers under different shear stresses. L. pneumophila, located at the bottom of the biofilm, remains surface-attached after biofilm detachment and seems to enhance the cohesiveness of these layers compared to P. fluorescens biofilms. On the contrary, when Legionella is not present, biofilm detachment increases with the increase of applied shear forces. All tested rotational velocities triggered L. pneumophila to enter the VBNC state in the bulk phase, while biofilm-associated VBNC cells were only observed at 400 RPM.

Finally, the contribution of the present work to *Legionella* control practices in water systems is discussed, highlighting the important insights that biofilms can provide in this context.

1. Introduction

Effective hydraulic management is critical for controlling *Legionella* in water systems [1,2]. Well-designed systems can reduce stagnation and biofilm formation by incorporating recirculation loops and eliminating dead ends, which, combined with strict control of flow velocity or temperature, can lower the risk of *Legionella* colonization and detachment [2]. However, biofilms serve as reservoirs for *Legionella*, and detachment events triggered by resumed flow after stagnant periods can release significant bacterial loads into bulk water, posing health risks [3, 41].

Biofilm detachment plays a major role in *Legionella* dissemination [5, 6]. Turbulent conditions, for instance, can cause substantial sloughing

events, releasing up to 90 % of *Legionella* cells into bulk water, and potentially exposing humans to infectious doses [7]. Recent studies have shown that neglecting biofilm detachment can lead to a severe underestimation of *Legionella* concentrations in engineered water systems by as much as 5.5 logs [8]. This underscores the importance of understanding biofilm detachment to effectively mitigate health risks associated with waterborne pathogens [9].

Bédard et al. [4] reported that short stagnation periods can lead to increased cell levels in the bulk, and a sudden increased flow of water can promote biofilm detachment and higher culturable levels of *Legionella* in the water. Also, Nisar et al. [10] demonstrated that intermittent water stagnation impacts both culturable and viable but non-culturable (VBNC) *Legionella* populations. They observed that

E-mail address: aalex@fe.up.pt (A. Pereira).

^{*} Corresponding author. LEPABE - Laboratory for Process Engineering, Environment, Biotechnology and Energy, Faculty of Engineering, University of Porto, Rua Dr. Roberto Frias, 4200-465 Porto, Portugal.

frequent flushing decreased culturable *Legionella* and led to an increase in VBNC cells.

Research has shown that *Legionella* may influence biofilm structure [11]. For example, spiking *Pseudomonas fluorescens* biofilms with *L. pneumophila* led to increased biofilm thickness under stagnant conditions [11]. The same study showed that *Legionella* predominantly localizes at the biofilm bottom layers, potentially offering protection during detachment events. Moreover, *Legionella*-biofilm interaction studies have shown that while low-flow conditions enhance *Legionella* adhesion to rough biofilm surfaces, higher shear stress promotes detachment from smoother biofilms [6]. Whether *Legionella* actively enhances biofilm cohesion remains unclear and warrants further study.

Therefore, studying biofilm detachment under varying hydrodynamic conditions is essential for understanding how maintenance practices influence Legionella spread and developing effective control strategies. To address these gaps, this study investigates the impact of resuming shear stress after a 48-h stagnation on biofilms colonized by L. pneumophila. The key research questions include: (a) Does shear stress affect the detachment of biofilms colonized by L. pneumophila? (b) What effect does shear stress have on the release of L. pneumophila into the bulk water phase? (c) Does shear stress trigger the transition of L. pneumophila into the VBNC state? For that, P. fluorescens biofilms were grown in a Center for Disease Control (CDC) biofilm reactor under 125 RPM (Reynolds number of 1552, turbulent regime), a well-characterized rotational speed [12], with L. pneumophila being spiked on day 3. On day 6, the system was subjected to stagnation for 48 h, after which the rotational velocity was resumed at 125, 225, or 400 RPM. A toolbox of mesoscale and microscale techniques was employed to study biofilms, and molecular approaches were used to determine Legionella viability.

Our results contribute to understanding the interactions between *Legionella* and biofilm structure, demonstrating that *Legionella*-colonized biofilms exhibit increased resilience to detachment compared to *P. fluorescens* biofilms alone. This study offers critical information that could enhance strategies for managing biofilms and *Legionella* in engineered water systems.

2. Materials and methods

2.1. Bacteria cultivation

P. fluorescens ATCC 13525^T (*Pf*) was used as the biofilm-forming microorganism in this study, as it is commonly found in water environments alongside *Legionella* species [13,14]. *Pf* was cultured overnight in R2 medium, which contains, per liter, 0.5 g peptone, 0.5 g glucose, 0.1 g magnesium sulfate \cdot 7H₂O, 0.3 g sodium pyruvate, 0.5 g yeast extract, 0.5 g casein hydrolysate, 0.5 g starch soluble, and 0.393 g di-potassium \cdot 3H₂O (Merck, Portugal). The culture was incubated at 30 °C and 120 RPM. *L. pneumophila* WDCM00107 (*Lp*) was selected for the experiments and cultured on buffered charcoal-yeast extract (BCYE) agar, prepared according to ISO 11731:2017 (Merck, Portugal).

Cultures were incubated at 37 °C for 2 days. Lp is responsible for approximately 90 % of legionellosis cases, making it the focus of this study. Furthermore, previous work demonstrated that Lp and Pf can coexist within biofilms [11].

2.2. Biofilm formation

2.2.1. Biofilm setup

The biofilm formation platform used in this study was the CDC Biofilm Reactor (Biosurface Technologies, USA). This device was chosen due to its standardization and previous use in studying the interaction between *Legionella* and biofilms in potable water under moderate to high fluid shear [12,15]. It offers precise control over the hydrodynamic conditions [12,16]. The bioreactor consists of a 1-liter glass beaker with eight polypropylene rods suspended from a ported lid. Each rod holds three circular polyvinyl chloride (PVC) coupons with a 1.27 cm diameter

(Neves & Neves, Portugal), positioned perpendicular to a rotating baffle. PVC was selected because it is commonly found in water systems and supports *Legionella* persistence.

2.2.2. Coupon preparation

Coupons were cleaned following the procedure outlined in ASTM E2871. Briefly, the coupons were sonicated in a 10 % (w/v) sodium dodecyl sulfate (SDS) solution (VWR International, Portugal) for 5 min. To ensure complete removal of any residual detergent, the coupons were rinsed with tap water and then sonicated again in ultrapure water. After rinsing thoroughly in ultrapure water, the coupons were air-dried and sterilized under ultraviolet (UV, 254 nm) radiation for 30 min. Meanwhile, the CDC biofilm reactor was also sterilized, and the cleaned coupons were aseptically placed onto the reactor rods.

2.2.3. Biofilm cultivation

On day 0, the bioreactor was inoculated with 1 mL of an overnight Pf culture (10^8 CFU/mL) in 500 mL of R2 medium. The baffle was set to rotate at 125 RPM ($0.0205~\text{N/m}^2$), a velocity previously characterized by computational fluid dynamics (CFD)[12]. Additionally, the authors investigated the influence of coupon position or holder on biofilm thickness, finding no significant differences at this rotational speed (data not shown).

The bioreactor was operated in batch mode for 24 h at room temperature. Following this, continuous flow was initiated for a total of 8 days, using a 1:10 dilution of R2 medium at a flow rate of 5 ± 0.5 mL/min, resulting in a residence time of 70 min [17]. No disinfectant was introduced during continuous operation. For the mixed biofilms (Pf + Lp), a suspension of Lp (10^9 CFU/mL) was prepared with sterile distilled water and introduced into the bioreactor on day 3. The continuous flow was interrupted for 2 h to allow for Lp settlement in the biofilm, after which the flow was resumed. Control experiments, which did not include the Lp spike, were also conducted. A control consisting of Lp-only biofilms was performed. For that, the CDC reactor was inoculated with an Lp suspension on day 0, and no Pf was added to the system.

2.3. Detachment

On day 6, the rotational velocity of the bioreactor was paused for 48 h while maintaining continuous flow. After the stagnation period, the rotational speed was restored to (a) 125 RPM, (b) 225 RPM, and (c) 400 RPM for 1 h. The hydrodynamic conditions corresponding to each rotational velocity are detailed in Table 1.

2.4. Biofilm analysis

The biofilms (both control and mixed) were sampled on days 6 and 8 after the 48-h stagnation period. Biofilm samples were then collected at time points of 5, 10, 15, 30, 45 min, and 1 h following the resetting of the rotational velocity. Bulk water samples (the suspension in contact with the biofilm) were also collected at the specified intervals. Coupons removed from each rod were rinsed twice with sterile saline solution (8.5 g/L NaCl, VWR International, Portugal) to remove any loosely attached cells. Coupons designated for OCT imaging were placed in a sterile 12-well microtiter plate (VWR International, Portugal), with each

 $\begin{tabular}{ll} \textbf{Table 1}\\ \textbf{Hydrodynamic parameters of the CDC biofilm reactor under different rotational velocities.} \end{tabular}$

Rotational Velocity (RPM)	Shear Stress (N/ m²)	Velocity (m/s)	Reynolds number	Hydrodynamic Regime
125 225	0.0205 0.0573	0.0571 0.1027	1552 2794	Turbulent Turbulent
400	0.1568	0.1826	4966	Turbulent

well filled with 3 mL of sterile saline solution. After OCT imaging, the saline solution was discarded, and the coupons were allowed to air dry. For biofilm cell quantification, two coupons were aseptically transferred to 50 mL Falcon tubes containing 5 mL of saline solution for disaggregation. Each Falcon tube underwent three alternating cycles of 30 s of low power sonication (Ultrasonic Cleaner USC-T, 45 kHz, VWR International, Portugal), followed by 30 s of vortexing.

2.4.1. Optical coherence tomography (OCT)

Biofilms were imaged using spectral-domain Optical Coherence Tomography (OCT; Thorlabs Ganymede, Thorlabs GmbH, Germany) according to the method described by Silva et al. [11]. The imaging volume was $2.49 \times 2.13 \times 1.52$ mm. For each coupon, at least six 2D images were captured, and three or more 3D image stacks (comprising 509 individual stacks) were acquired. The images were processed using the Biofilm Imaging and Structure Classification Automatic Processor (BISCAP software), where pixel intensity thresholds were applied to distinguish biomass from the liquid phase by binarizing the pixels into either biomass or background [18,19]. Biofilm thickness, defined as the distance from the top to the bottom of the biofilm, and porosity, the fraction of void spaces within the biofilm, were quantified using BISCAP. Representative 3D-OCT images were chosen for each condition (before, 5 min, and 1 h after resuming the shear – mixed biofilms) and videos were generated using 200 of the 509 stacks with Fiji software.

2.4.2. Confocal laser scanning microscopy (CLSM)

The spatial location of Lp within the Pf biofilms on day 8 before and after resetting the rotational velocity to 125, 225, or 400 RPM was tracked at the specified time points (section 2.4). Lp was stained red using molecular tools (16S rRNA PNA probe, PLPNE620) as previously described[11,20]. Samples were examined with a helium-neon laser at 565 nm and a 405-diode at 398 nm, using a $60 \times glycerol$ objective lens (Leica HC PL APO CS, Leica Microsystems, Germany) on an inverted Leica DMI6000-CS microscope.

For each biofilm sample, a minimum of three z-stacks of horizontal plane images (512 \times 512 pixels, covering 387.5 \times 387.5 μm) with a z-step of 0.36 μm were acquired. In the confocal images, green represents Pf cells, due to their auto-fluorescence[21], and red indicates Lp. Three-dimensional (3D) projections of biofilm structures were created from z-stacks using the "Easy 3D" tool in IMARIS 9.1 software (Bitplane, Switzerland), and orthogonal views were also generated. Biovolume (the total biomass volume, μm^3 , per unit area, μm^2) for each bacterium was quantified with the COMSTAT2 plugin for ImageJ.

2.4.3. Quantification of sessile and planktonic cells

The disaggregated biofilm suspensions and bulk water samples were heated to 50 °C for 30 min to eliminate Pf from the sample and then spread onto BCYE-GVPC (buffered charcoal yeast extract with glycine, vancomycin, polymyxin, and cycloheximide) selective agar medium. Plates were incubated at 37 °C for up to 10 days.

To determine the number of PNA-positive Lp cells, a FISH assay was conducted using the referred PNA probe. In brief, 25 μ L of a suitable dilution (of biofilm suspension or bulk water) was placed on the wells of hybridization slides and allowed to air dry. The slides were flamed three times, treated with 90 % (v/v) ethanol, and air-dried to fix the cells. Hybridization and washing were carried out according to Wilks et al. [20]. After the FISH procedure, slides were air-dried, a drop of non-fluorescent immersion oil (Sigma, Portugal) was added, and a coverslip was placed over the sample. A second drop of immersion oil was applied to the objective, and slides were observed using a Nikon Eclipse Ti SR inverted epifluorescence microscope (Nikon Instruments, Netherlands) with 40 \times Plan APO objectives (Nikon Instruments). Images were captured using a DS-Ri2 camera (Nikon Instruments).

2.4.4. Viable but nonculturable (VBNC) Lp

Direct viable count (DVC) - FISH technique was used to quantify Lp

VBNC cells. One milliliter of the biofilm or bulk sample was added to 4 mL of sterile distilled water and 5 mL of R2 medium. Pipemidic acid, an antibiotic that inhibits cell division, was added to a final concentration of 10 $\mu g/mL$. Samples were then incubated overnight at 37 $^{\circ}C$ with agitation. Following incubation, samples were hybridized and observed under the microscope as described previously (section 2.4.3). Cells that had elongated to at least twice their original size were considered viable. The percentage of VBNC cells was calculated as the difference between the viable cell count and culturable cell count relative to the total Lp cell count, as shown in the equation below.

$$\text{%VBNC} = \frac{\text{Viable cells} - \text{CFU}}{\text{Total cells}} \times 100$$

2.5. Statistical analysis

The data were analyzed using GraphPad Prism 9.0 for Windows (GraphPad Software, USA). All experiments were performed in three independent replicates.

Each experimental condition was assessed in duplicate within each trial, and each experiment was independently repeated three times to ensure reproducibility. For each parameter evaluated, the values from the technical replicates were first averaged to obtain a single value per experiment. Then, the mean values were combined across the three independent experiments (biological replicates), and the overall mean and standard deviation (SD) were calculated. Statistical significance was determined by applying one-way analysis of variance (ANOVA) when comparing multiple groups. Pairwise comparisons between two groups were conducted using the Student's t-test. A stringent significance threshold was set at p < 0.0005.

3. Results

3.1. Biofilm characterization during stagnation

No significant differences were found for the quantitative structural parameters between biofilms from days 6 (before initiating stagnation, data shown in Supplementary Material) and 8 (48 h after stagnation).

Fig. 1(A and B) shows representative 2D – OCT images of the control (P. fluorescens alone, Pf), mixed (P. fluorescens biofilms spiked with L. pneumophila, Pf + Lp) and Lp-only biofilms on day 8, after the 48-h stagnation period. The spatial location of L. pneumophila, marked in red with a PNA probe, within biofilms, can be seen in the CLSM images (Fig. 1c and d). Quantitative biofilm structural parameters for each condition are summarized in Table 2.

The control of Lp biofilm did not present any mesoscale structure visible under the OCT (Fig. 1e). The 2D – OCT mesoscale images of control (Pf) and mixed (Pf + Lp) biofilms after the 48-h stagnation period point out different structures. Fig. 1(a and b) shows that the Pf + Lp biofilms are significantly thinner and have a more irregular surface compared to the control biofilms. This is corroborated by data in Table 2, which further suggests that biofilms with Lp have higher porosity and lower compaction. The video provided in the Supplementary Material (SM1 – Before, for example, by 10 s) highlights the porosity of the mixed biofilms by showing several water-filled areas (marked in blue and distributed along the whole biofilm structure) as well as its irregular surface.

Complementary, the CLSM microscale analysis of the mixed biofilms revealed that Lp was predominantly located at the bottom of the biofilm (as confirmed by data provided in Supplementary Material concerning Lp quantification per biofilm layer), but not uniformly distributed, as shown in the confocal images (Fig. 1, panels c and d). Very bright and intense clumps of Lp were observed with thinner layers of bacteria.

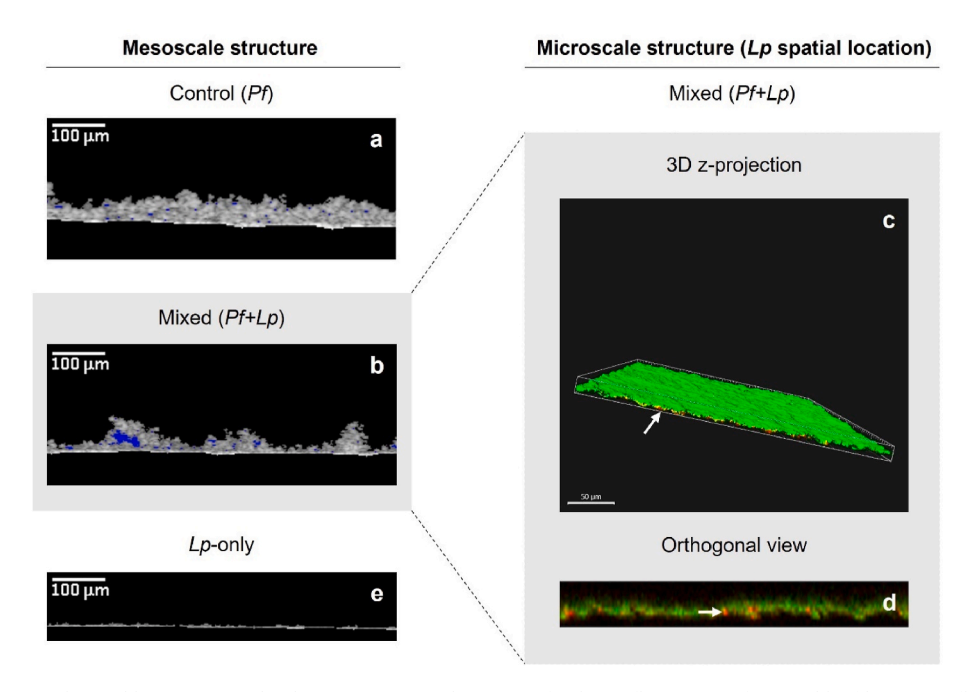


Fig. 1. Representative images obtained by 2D – Optical Coherence Tomography (OCT) of 8-day *P. fluorescens* (*Pf*) control biofilms (a), *P. fluorescens* spiked on day 3 with *L. pneumophila* (*Pf* + *Lp*) (b), and *Lp*-only biofilms (e). The water-filled spaces within the biofilm structure are colored blue. Representative CLSM images of the mixed biofilm (right, panels c – 3D z-projection and d – orthogonal view), with *L. pneumophila* stained in red using a 16S rRNA PNA probe. The white arrow indicates *Lp*. The presented projections were obtained using IMARIS, and the white scale bars are 50 μ m. (For interpretation of the references to color in this figure legend, the reader is referred to the Web version of this article.)

Table 2 Quantitative structural parameters of 8-days (after 48 h of stagnation) of the control P. fluorescens (Pf) and mixed (Pf + Lp) biofilms of P. fluorescens and L. pneumophila.

Day 8	Thickness	Porosity	Compaction Parameter	Roughness Coefficient
Control (Pf) ^c	41 ± 6	0.13 ± 0.05	0.87 ± 0.03	0.42 ± 0.07
$\begin{array}{c} \text{Mixed } (Pf \\ + Lp)^{\text{c}} \end{array}$	25 ± 4^a	0.25 ± 0.08^a	0.79 ± 0.04^a	0.51 ± 0.04^b

^aStatistically significant differences between the mixed and the control biofilms are represented for p < 0.0005 by ***.

3.2. Effect of imposing shear on the biofilms after stagnation

After 48 h of stagnation, the biofilms were suddenly exposed to shear stresses. Three different rotational speeds were independently evaluated: (a) 125 RPM, (b) 225 RPM, and (c) 400 RPM on day 8.

3.2.1. Biofilm structural variations and Lp distribution

The quantitative analysis (thickness and porosity) of the mesoscale structure of biofilms prior to and 5, 10, 15, 30, 45 min, and 1 h after increasing the shear stress are presented in Fig. 2.

Fig. 2 shows that the thickness of the biofilms colonized by Lp (mixed – grey bars) significantly decreased (about 50 %, p < 0.0005) after being subjected to the different rotational velocities (125, 225, and 400 RPM). In all cases, the significant thickness decrease was found in just 5 min, remaining fairly constant for the 1-h period. The average thickness after the shear stress (between 5 min and 1 h) is 12 ± 2 , 16 ± 5 and 12 ± 2 μ m for 125, 225 and 400 RPM, respectively. In contrast, the control biofilm (Pf alone) was affected differently by the different rotational speeds. At 125 RPM, no thickness reduction was observed, but as the rotational

velocity increased, the thickness progressively decreased, with the biofilm thickness below the detection limit at the mesoscale under 400 RPM. For clarification, an additional control of Lp biofilms spiked by day 3 with Pf was accomplished (data shown in Supplementary Material). Under this scenario, it was found that by day 3 (before Pf spiking), Lpbiofilms did not present a mesoscale structure, even though Lp was attached to the coupons' surface (red-Lp cells were observed in the CLSM, and CFU accounted for $4.8 \log_{10}$ CFU/cm²).

Similarly to what was found for the thickness, the porosity of the mixed biofilms significantly decreased (from 0.24 \pm 0.06 to 0.17 \pm 0.03, p < 0.0005) 1 h after the shear stress was imposed. That might be a consequence of the detachment of the upper-middle biofilm layers, where many water-filled spaces could be seen (SM1 video). The control biofilms exhibited a different response. At 125 RPM, there were no changes in porosity (consistent with the lack of thickness variation), but at 225 RPM, the biofilm thickness decreased while porosity increased (0.14 \pm 0.04 to 0.25 \pm 0.04, p < 0.0001), indicating a less compact structure after detachment. For all tested conditions, such changes were observed right after (5 min) the rotational velocity increase and were kept stable until the 1-h mark.

The mesoscale structure of biofilms after shear stress was imposed was also evaluated qualitatively (Fig. 3a-c, e) and combined with microscale analysis to track *Lp* distribution within the biofilm through confocal microscopy (Fig. 3b-d, f).

The 2D – OCT images of the mixed biofilms (Pf + Lp) from Fig. 3 clearly show the previously discussed thickness reduction observed 1 h after the rotational velocity was imposed, in comparison to the initial biofilm (Fig. 1b). The videos supplied in SM (referring to the tested condition of 225 RPM) also provide valuable information on variations in biofilm structure. In general, videos show that 5 min after re-setting the shear stress, the mixed biofilm's structure is very unstable (SM2 video), with several stacks of microcolonies. However, by the 1-h mark, the biofilms are still thin but with a more homogeneous surface (SM3 video)

The confocal images confirm that *Lp* remained in the biofilm structure regardless of the applied shear forces after the stagnation period.

^bStatistically significant differences between the mixed and the control biofilms are represented for p < 0.0001 by ****.

^cNo significant differences between biofilms from days 6 (data not shown) and day 8 were found.

A.R. Silva et al. Biofilm 10 (2025) 100323

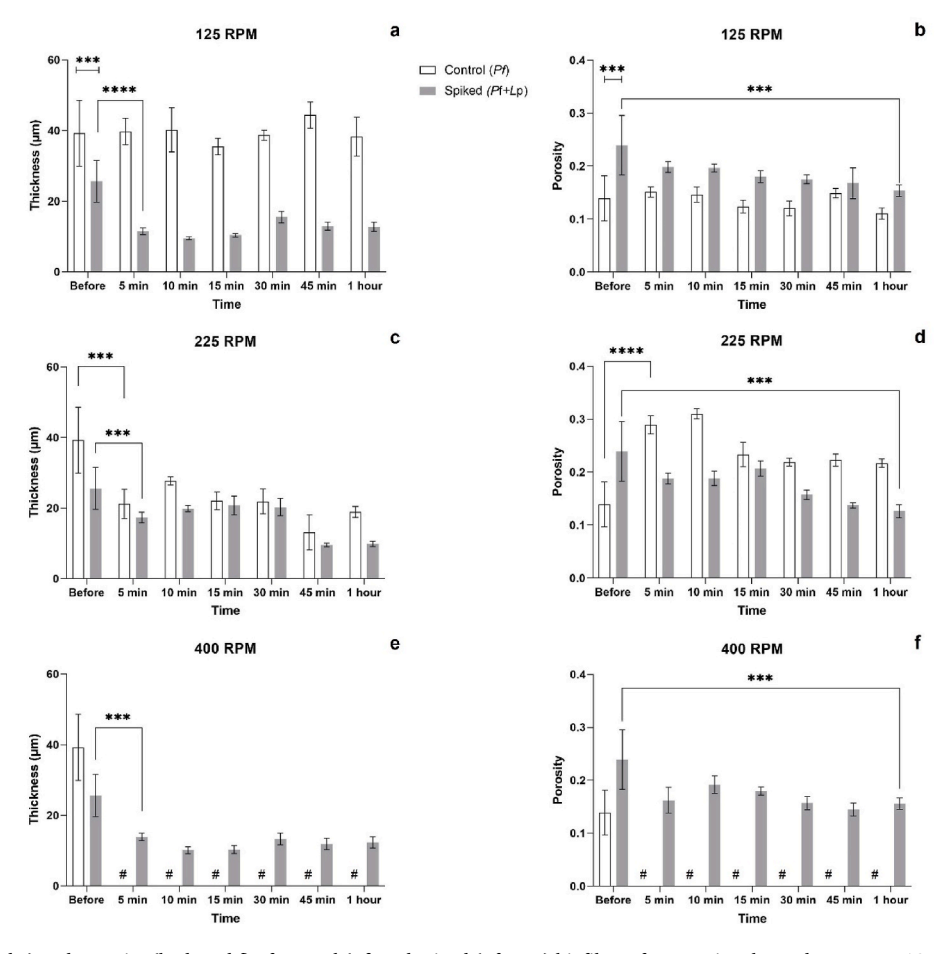


Fig. 2. Thickness (a, c and e) and porosity (b, d, and f) of control (Pf) and mixed (Pf + Lp) biofilms after rotational speed was set to 125 RPM (a and b), 225 RPM (c and d), and 400 RPM (e and f). The mean \pm standard deviation is shown. No bars are shown for the control biofilm for the 400 RPM since those are below the detection limit (#). Statistically significant differences are represented for p < 0.0005 by *** and <0.0001 by ****. The parameters were quantified through the analysis of 3D – OCT images with BISCAP software.

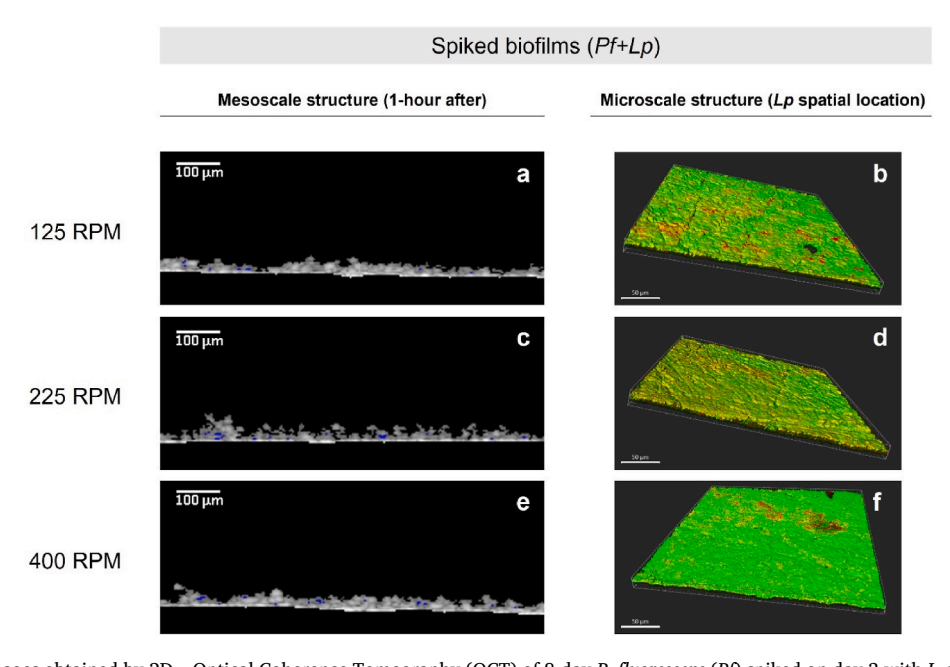


Fig. 3. Representative images obtained by 2D – Optical Coherence Tomography (OCT) of 8-day P. fluorescens (Pf) spiked on day 3 with L. pneumophila (Pf + Lp) (a, c and e) 1 h after imposing the rotational velocity. The water-filled spaces within the biofilm structure are colored blue. Representative CLSM images of the mixed biofilm (right, b, d, and f - 3D z-projection), with L. pneumophila stained in red using a 16S rRNA PNA probe. The presented projections were obtained using IMARIS. (For interpretation of the references to color in this figure legend, the reader is referred to the Web version of this article.)

The confocal images (Fig. 3b–d and f) specifically highlight the spatial location of *Lp*, which seems to be now more present in the middle-upper layers (as confirmed by the quantification of *Lp* location, data shown in Supplementary Material).

Additionally, the biovolume of *Lp* in the mixed biofilms (Fig. 4) was determined by CLSM before and 1 h after shear increase.

The biovolume of Lp in the mixed Pf + Lp biofilms increased after the shear stress was re-applied (from 5.92 ± 0.98 to $11.01 \pm 2.22 \ \mu m^3/\mu m^2$). The biovolume of Pf in mixed biofilms was quantified before and 1 h after shear stress was resumed, with no significant changes observed (see Supplementary Material). In the context of our study, the biofilm appears to reorganize to counteract detachment forces, becoming more compact and cohesive. This compaction reduces porosity and likely enhances the retention of Legionella, increasing its biovolume. These observations likely reflect the readjustments of Lp within the biofilm, and are not derived from any changes in the Pf biovolumes.

3.2.2. Legionella in VBNC

The culturability (colony-forming units, blue line), PNA-positive cells (PNA-FISH assay, black line), and VBNC cells (DVC-FISH assay, expressed as percentage values) of *L. pneumophila* in the bulk and the biofilm are presented in Fig. 5.

Fig. 5 shows that very high numbers of PNA-positive *Lp* cells (black lines) were observed over the 1 h for all the tested rotational velocities, either in biofilm or bulk. The contribution of *Lp* detachment to the bulk water does not seem to significantly affect the numbers formerly observed.

The numbers of PNA-positive Lp cells (FISH-assay, black lines) were significantly higher (p < 0.0001) than the numbers of cultivable cells (blue line). No significant differences exist in the culturable numbers of Lp-biofilm for the 125 and 225 RPM conditions (p < 0.0005). However, for the 400 RPM, a total loss of culturability was observed for the Lp in the biofilms, which is consistent with the decrease in Lp biovolume. On the other hand, a total loss of culturability was observed for Lp in the bulk, regardless of the rotational velocity imposed. The loss of culturability was associated with a shift to the VBNC state, namely in the bulk before and 1 h after shear stress (16 % vs 81 %, respectively – Fig. 5a). Similarly, the loss of culturability of the Lp-biofilm observed for the highest rotational velocity (400 RPM) increased the VBNC population (before and 5 min after shear stress, from 13 % to 88 %, respectively). Interestingly, the culturable numbers of Pf in the mixed biofilms

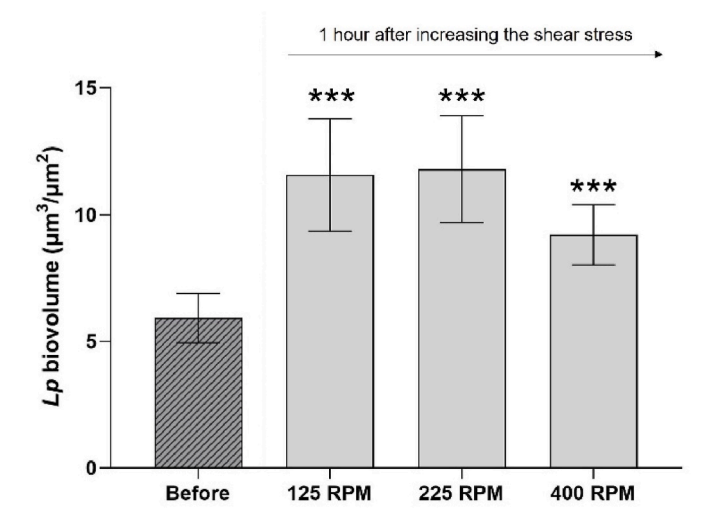


Fig. 4. Biovolume of *L. pneumophila* (*Lp*) in mixed biofilms (Pf + Lp) before and 1 h after the shear stress was resumed. Values were extracted from confocal images with the COMSTAT plugin. The means \pm standard deviations are shown. Statistically significant differences are represented for p < 0.0005 by *** when compared to before increasing the shear stress.

remained fairly constant, despite the detachment of the upper layers of the biofilm.

4. Discussion

Water systems frequently experience shifts in hydraulic conditions, ranging from stagnant water (no flow) to sudden changes in flow regimes [22]. These shifts, particularly from stagnation to flow, arguably represent an increased public health risk associated with Legionnaires' disease. Increased shear forces can cause biofilm detachment, releasing high concentrations of *Legionella* to the bulk water. This study addresses a critical knowledge gap by investigating how flow shifts affect biofilm detachment and the subsequent distribution of *L. pneumophila* between the bulk and the biofilm.

4.1. How shear stress affects biofilm detachment and Lp release to the bulk phase

The present study demonstrates that biofilms colonized by Lp (mixed, Pf + Lp) exhibit greater resilience to shear shifts compared to control Pf biofilms (Figs. 2 and 3), thus keeping the basal layer integrity. In both cases, imposing a rotational speed on the biofilms after stagnation generally led to a significant reduction in thickness for all three tested shear stresses (125, 225, and 400 RPM, corresponding to Reynolds numbers of 1552, 2794, and 4966, respectively). However, for the mixed biofilms, similar thickness reductions of approximately 50 % (Fig. 2) were observed for all three rotational speeds (over 1 h), suggesting that the presence of Lp strengthens the cohesiveness of the biofilm's bottom layers.

The decrease in biofilm porosity (Fig. 2) further supports this idea. Lp is predominantly located at the bottom of the biofilm (Fig. 1), where low oxygen areas are found [23]. As suggested by Silva et al. [11], Legionella's preference for low-oxygen environments, combined with the oxygen demands of P. fluorescens, promotes a spatial rearrangement within the biofilm matrix that benefits both bacteria - increased water-filled areas in the top layers and lower in the bottom ones (more compact regions) (Fig. 1). The decrease in biofilm porosity and Lp biovolume increase in the mixed biofilms suggests enhanced cohesion and compaction, particularly in the basal layers (as observed in SM3 video, where most of the water-filled spaces were located at the upper part of the biofilm - sec 12). The concept of biofilm layering, where a robust basal layer offers structural integrity, has been described by several authors [24-27]. Indeed, Rochex et al. [26] and Paul et al. [25] reported a stratified biofilm structure, with a thin and cohesive basal layer capable of resisting shear stress, while the upper layer is more susceptible to detachment. Silva et al. [28] similarly observed this layered structure, noting that biofilm upper layers detached during thermal disinfection under varying shear stresses, leaving a stable basal layer

These observations suggest that the increased biofilm stability is likely driven by species-specific interactions. Legionella colonization appears to alter biofilm structure through mechanisms that increase cohesion and structural integrity in the basal layers, enhancing resistance to detachment forces. The results from the present study align with findings in other research, which demonstrated that pathogen colonization can affect the host cohesion and resistance to shear stress. For example, Mikaty et al. [29] observed that Neisseria meningitidis microcolonies on host cell surfaces exhibit cohesion due to bacterial interactions as well as host cellular responses that form stabilizing structures, enhancing microcolony stability against drag forces from blood flow. Moreover, studies on other mixed-species biofilms, such as those with Pseudomonas aeruginosa or Staphylococcus aureus, have shown that pathogenic bacteria can enhance biofilm cohesion, leading to more robust structures, particularly through EPS production, which fortifies the basal structure and reduces susceptibility to detachment [30,31]. Given that, it is not surprising that the *Pf* biofilms (control, without *Lp*)

A.R. Silva et al. Biofilm 10 (2025) 100323

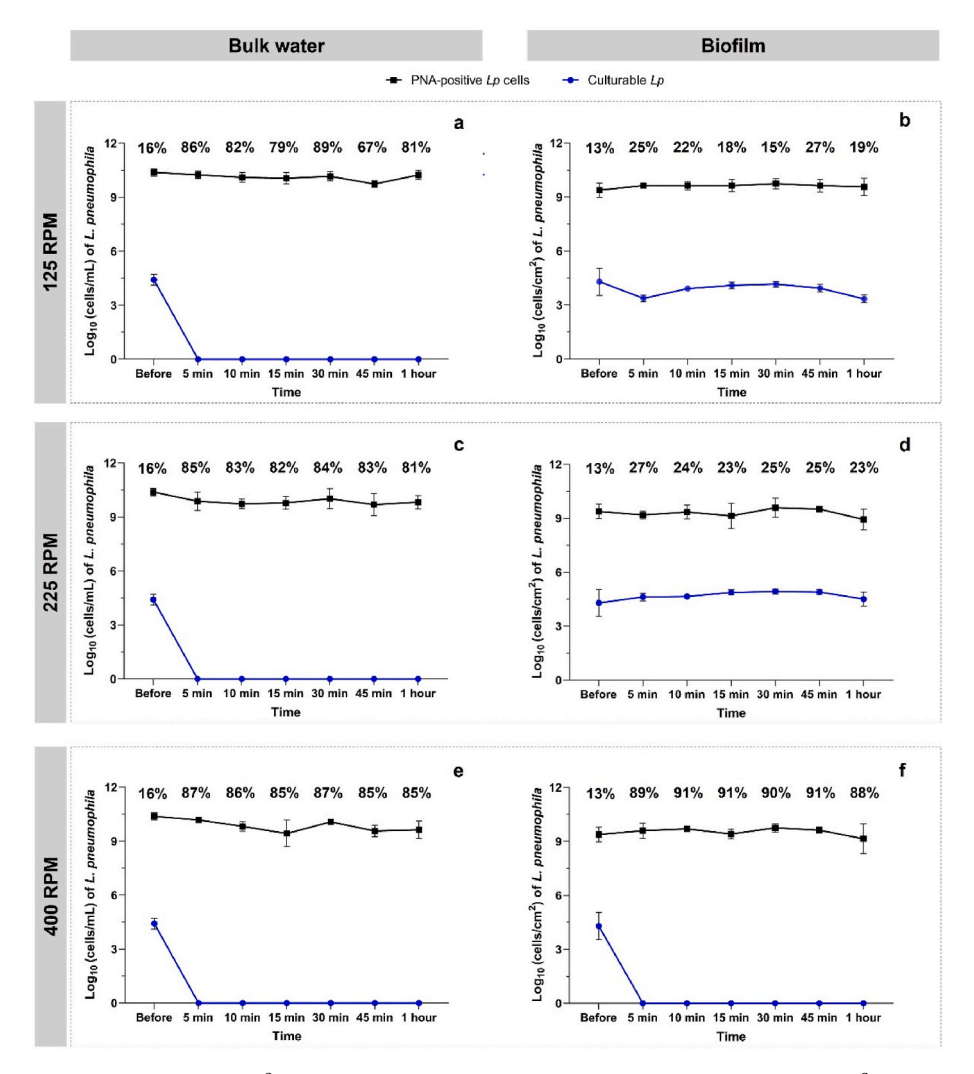


Fig. 5. The number of culturable (CFU, \log_{10} CFU/cm² or mL) and PNA-positive cell counts of *L. pneumophila* (*Lp* cells/cm²) over the 1-h period of shear stress increase in the bulk water (left side; bulk water refers to the suspension in contact with the biofilm) and in biofilm (right side). The percentages of the *L. pneumophila* population in VBNC are shown for each timepoint and were calculated considering the culturable and the total *L. pneumophila* cell counts. The mean \pm standard deviation is shown. Statistically significant differences are represented for p < 0.0005 by ****

detachment is dependent on the shear stress imposed, ranging from almost no detachment at 125 RPM, to 45 % detachment at 225 RPM, and almost complete detachment of the mesoscale structure of control biofilms at 400 RPM.

Similar findings were previously reported. For example, under simulated microgravity conditions, *S. gordonii* biofilms increased biovolume and exhibited extensive chaining of cells, suggesting an adaptive response to environmental stress [32].

Interestingly, despite biofilm detachment, no significant (p>0.05) concentrations of Lp were released into the bulk phase – before and 1 h after shear increase – at any shear stress (Fig. 5, PNA-positive Lp cells). This is arguably the consequence of Lp spatial positioning inside the biofilm matrix and follows former observations from Meegoda et al. [33] who reported that flushing in a pilot-scale premise plumbing system had minimal impact on Legionella spp. total counts in pipe wall biofilms.

Finally, it is important to note that in the present study, Lp was spiked only once (on day 3), and nutritional medium was continuously supplied to the bioreactor at a flow rate of 5 mL/min. Legionella seems to be able to grow under the experimental conditions of the present study, as both PNA-positive and CFU Lp counts remained relatively stable (9 and 4 log_{10} , respectively) over the 8 days (data shown in Supplementary Material). Otherwise, Lp in the bulk would be washed out of the system within a couple of hours, given the setup's residence time of 70 min and

washout kinetics [17]. One might also note that the presence of disinfectant and/or free-living amoeba could have led to different findings.

The variability between independent biological replicates was consistently low (low error bars). Previous studies have shown that the CDC biofilm reactor, when operated under well-controlled conditions, produces highly reproducible single-species biofilms (such as those of P. fluorescens, P. aeruginosa, etc.) [12,28,34]. In this study, P. fluorescens biofilms were grown and later colonized by L. pneumophila. The low variability observed in the present work is consistent with other studies that have been reporting reproducible models concerning multi-species biofilms [35–37]. For example, An et al. [35] developed a reproducible model system of the complex oral microbiota using a CDC biofilm reactor. Armbruster et al. [38], using a multi-species biofilm model, reported a between-experiment variance of 0.0316 and observed no significant differences in the mean biofilm cell densities across three independent Other studies experiments. former P. fluorescens/L. pneumophila biofilms also reported low inter-replicate errors concerning the biofilm structure and CFU counts [11,39], supporting the observations of the present study.

4.2. Does shear stress trigger a VBNC response in L. pneumophila?

Results demonstrate that Lp in the bulk phase is more susceptible to

enter the VBNC state under sudden shear stress compared to biofilm-associated Lp (Fig. 5). This observation highlights the protective role of biofilm structures, which shield bacteria from environmental stressors more effectively than when they are in a planktonic state [40,41]. These findings are consistent with former studies that shows the resilience of biofilms even under high shear stress or after remedial actions as flushing [10,42].

While *Lp* rapidly lost culturability in the bulk phase (within 5 min, Fig. 5) across all shear conditions, it maintained its culturability in the biofilm. However, at the highest rotational velocity (400 RPM), even biofilm-associated *Legionella* lost culturability within 5 min, suggesting that the increased shear stress can overcome biofilm protection (Fig. 5e).

Concerning the VBNC population, the current findings indicate that shear stress might be among several environmental triggers that can prompt Lp to enter the VBNC state. Formerly, Nisar et al. [10] showed that regular flushing, while effective at reducing culturable populations, has been linked to increases in VBNC cells. Besides, numerous studies have shown that exposure to disinfectants such as monochloramine and chlorine dioxide can drive L. pneumophila into VBNC states [43-46], which can remain infective in animal models [47]. For example, Alleron et al. [44] reported that VBNC Legionella populations induced by monochloramine persisted in biofilms for at least four months. Farhat et al. [48] showed the persistence of VBNC Legionella in biofilms after heat shock in a simulated hot water system. Other factors, such as nutrient starvation [49] and material properties, such as copper piping [50,51], also enhance VBNC transitions. These findings collectively emphasize the ability of Legionella to survive environmental stressors in a VBNC state. Finally, the pre-treatment required for BCYE culture could lead to the loss of viable culturable Legionella cells, potentially affecting the VBNC numbers.

A conceptual model of how *Lp*-colonized *Pf* biofilms behave to shear stress was proposed (Fig. 6).

The bottom-layer spatial location of Lp was consistently observed across the biological replicates, in agreement with other former studies [11,39]. This distribution likely reflects the specific nutritional and physiological requirements of the two species; in particular, the microaerophilic nature of Lp favors its presence in the bottom layers of the biofilm [23]. Furthermore, the mechanism described was consistently observed in the three independent experiments, since Lp remained biofilm-attached for all the tested shear stresses.

5. Contributions of the present study to *L. pneumophila* control practices at water systems

5.1. Stagnation period: impact on biofilms and L. pneumophila

The biofilm structural properties and the amount of Lp (measured by total and culturable cells – Figs. 1 and 5) were not significantly changed after 48 h of stagnation. Although stagnation alone is typically associated with increased Legionella risk, the effective risk is always a function of the combined effect of several parameters, such as: hydrodynamics, surface material, water quality, among others. This aspect is clearly

addressed by Rhoads et al. [52] who, while studying the effect of reduced water demand on *L. pneumophila* occurrence in buildings, reported that stagnation alone does not necessarily lead to an increase in *Legionella* concentrations, suggesting that the pipe length and the temperature profiles should be taken into consideration as contributors to *Legionella* growth in building systems [53,54].

5.2. L. pneumophila remains attached to the surface after biofilm detachment and quickly shifts to VBNC state in the bulk

Worldwide *Legionella* control practices in water systems rely on discrete water sampling for bacteria quantification, disregarding the role of biofilms [55,56].

In the present study, most Lp remained attached to the surface, despite the removal of the outer biofilm layers (Fig. 3). This reinforces that $\mathit{Legionella}$ is very difficult to eradicate from water systems once it enters such systems, justifying its widespread presence across water systems [55]. It also points out that water-focused monitoring programs underestimate the true concentrations of $\mathit{Legionella}$ in the systems. This is further aggravated by the fact that a simple flow increase, after a 48-h stagnation period, is enough to bring a significant amount of $\mathit{Legionella}$ population in the bulk (\approx 80 %) to the VBNC state.

The present work is not focused on a real-field experiment; however, in a scenario where a shower has been stagnant over the weekend and then sampled, most of the *Legionella* population in the bulk water would likely be undetectable by culturing. This further highlights the ongoing discussion about the limitations of culture methods, the gold-standard for *Legionella* routine monitoring advocated by most worldwide guidelines, particularly regarding the detection of VBNC cells [57]. These VBNC cells, although non-culturable, can still pose significant risks to public health, particularly since they may revert to a culturable and infective state under certain conditions [43,47].

5.3. The critical importance of biofilms for L. pneumophila settlement

The former discussions support a broader view that biofilms not only protect *Legionella* against environmental stress (like shear increases) but also serve as reservoirs for large amounts of *L. pneumophila* (including VBNC cells) that persist despite physical or chemical stressors.

Legionella in the remaining biofilm basal layer may now be more vulnerable to other control measures (e.g., biocides), but also facilitate faster microbial recolonization [58]. Future studies should consider the impact of chemical stressors.

There is still a long way to go, but it is important to start addressing biofilm analysis in a systematic way to provide valuable information for *Legionella* prevention practices in water systems. This work, apart from the findings already discussed, proposes a combined approach of meso-and microscale biofilm analysis tools coupled with microbiological analytical techniques (culture *vs* molecular methods), which can be used in future studies in real-field systems, combined for instance with genetic information [59].

Future studies should further elucidate the mechanisms by which

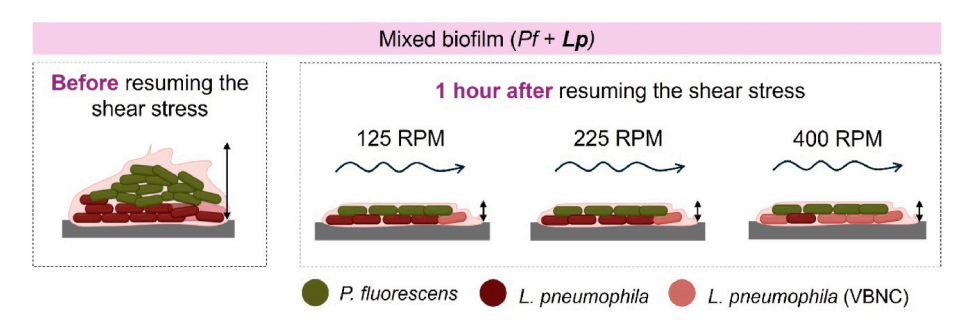


Fig. 6. Conceptual model regarding Lp-colonized biofilms response when the flow was resumed (to 125, 225, and 400 RPM) after a stagnation period.

species like *L. pneumophila* influence biofilm resilience to detachment, which could inform strategies for managing biofilm formation in environments where pathogenic biofilms pose risks. Furthermore, the limitations of this study comprise the use of a controlled biofilm model, which may not fully replicate the complexity of real-world water systems, where factors like water chemistry and microbial communities vary. Given that, the authors recognize that the present study does not mimic a real water system model, nor the real interactions found in field systems.

6. Conclusions

The detachment of *L. pneumophila* from biofilms presents a significant challenge in managing its risks within water distribution systems. Biofilm-associated *Legionella* can persist despite control measures and intermittently release bacteria into the water through sloughed biofilm portions. The main conclusions of this study are as follows:

- (i) L. pneumophila enhances the structural resilience of biofilms to detachment, particularly in the basal layers, where the pathogen remains in high concentrations even after biofilm detachment caused by increased shear stress.
- (ii) In the bulk phase, L. pneumophila rapidly shifts into a viable but non-culturable (VBNC) state in response to hydrodynamic shifts (from stagnation to shear stress). Planktonic cells are more susceptible to the shear increase than biofilm-associated cells. This increase in VBNC populations could lead to the underestimation of Legionella risks in water systems.

Effective management must account for the structural stability of the biofilms to reduce health risks associated with biofilm detachment and *L. pneumophila* dissemination into water systems.

CRediT authorship contribution statement

Ana Rosa Silva: Writing – review & editing, Writing – original draft, Methodology, Investigation, Formal analysis, Conceptualization. C. William Keevil: Writing – review & editing, Supervision. Ana Pereira: Writing – review & editing, Writing – original draft, Supervision, Funding acquisition, Conceptualization.

Declaration of competing interest

The authors declare that they have no known competing financial interests or personal relationships that could have appeared to influence the work reported in this paper.

Acknowledgements

This work was financially supported by national funds through FCT/MCTES (PIDDAC): LEPABE, UIDB/00511/2020 (DOI: 10.54499/UIDB/00511/2020) and UIDP/00511/2020 (DOI: 10.54499/UIDP/00511/2020) and ALiCE, LA/P/0045/2020 (DOI: 10.54499/LA/P/0045/2020); by national funds through the FCT/MCTES (PIDDAC), under the project 2022.03523.PTDC - LegioFilms - Understanding the Role of Biofilm Architecture in *Legionella* Colonization and Risk of Detachment in hospital networks using an Integrated Monitoring Approach, with DOI 10.54499/2022.03523.PTDC (https://doi.org/10.54499/2022.03523.PTDC). Ana Rosa Silva thanks the Portuguese Foundation for Science and Technology (FCT) for the financial support of the PhD grant (2020.08539.BD).

Appendix A. Supplementary data

Supplementary data to this article can be found online at https://doi.org/10.1016/j.bioflm.2025.100323.

Data availability

Data will be made available on request.

References

- [1] Bédard E, Boppe I, Kouamé S, Martin P, Pinsonneault L, Valiquette L, Racine J, Prévost M. Combination of heat shock and enhanced thermal regime to control the growth of a persistent *Legionella pneumophila* strain. Pathogens 2016;5:35. https://doi.org/10.3390/pathogens5020035.
- [2] Boppe I, Bédard E, Taillandier C, Lecellier D, Nantel-Gauvin M-A, Villion M, Laferrière C, Prévost M. Investigative approach to improve hot water system hydraulics through temperature monitoring to reduce building environmental quality hazard associated to legionella. Build Environ 2016;108:230–9. https://doi. org/10.1016/j.buildenv.2016.08.038.
- [3] Abdel-Nour M, Duncan C, Low DE, Guyard C. Biofilms: the stronghold of Legionella pneumophila. Int J Mol Sci 2013;14:21660–75. https://doi.org/10.3390/ jims141121660.
- [4] Bédard E, Laferrière C, Déziel E, Prévost M. Impact of stagnation and sampling volume on water microbial quality monitoring in large buildings. PLoS One 2018; 13:e0199429. https://doi.org/10.1371/journal.pone.0199429.
- [5] Declerck P. Biofilms: the environmental playground of Legionella pneumophila. Environ Microbiol 2010;12:557–66. https://doi.org/10.1111/j.1462-2020.2009.02025 x
- [6] Shen Y, Monroy GL, Derlon N, Janjaroen D, Huang C, Morgenroth E, Boppart SA, Ashbolt NJ, Liu W-T, Nguyen TH. Role of biofilm roughness and hydrodynamic conditions in *Legionella pneumophila* adhesion to and detachment from simulated drinking water biofilms. Environ Sci Technol 2015;49:4274–82. https://doi.org/10.1021/es505842v.
- [7] Storey MV, Ashbolt NJ, Stenström TA. Biofilms, thermophilic amoebae and Legionella pneumophila - a quantitative risk assessment for distributed water. Water Sci Technol 2004;50:77–82. https://doi.org/10.2166/wst.2004.0023.
- [8] Ortiz C, Hatam F, Prévost M. Uncertainty sources in the mechanistic modeling of legionella within building water systems. Eng Proc 2024;69:84. https://doi.org/ 10.3390/engproc2024069084.
- [9] Hemdan BA, El-Taweel GE, Goswami P, Pant D, Sevda S. The role of biofilm in the development and dissemination of ubiquitous pathogens in drinking water distribution systems: an overview of surveillance, outbreaks, and prevention. World J Microbiol Biotechnol 2021;37:36. https://doi.org/10.1007/s11274-021-03008-3.
- [10] Nisar MA, Ross KE, Brown MH, Bentham R, Best G, Eyre NS, Leterme SC, Whiley H. Increased flushing frequency of a model plumbing system initially promoted the formation of viable but non culturable cells but ultimately reduced the concentration of culturable and total legionella DNA. Heliyon 2024;10:e32334. https://doi.org/10.1016/j.heliyon.2024.e32334.
- [11] Silva AR, Melo LF, Keevil CW, Pereira A. Legionella colonization and 3D spatial location within a pseudomonas biofilm. Sci Rep 2024;14:16781. https://doi.org/ 10.1038/s41598-024-67712-4.
- [12] Johnson E, Petersen T, Goeres DM. Characterizing the shearing stresses within the CDC biofilm reactor using computational fluid dynamics. Microorganisms 2021;9: 1709. https://doi.org/10.3390/microorganisms9081709.
- [13] Stewart CR, Muthye V, Cianciotto NP. Legionella pneumophila persists within biofilms formed by Klebsiella pneumoniae, flavobacterium sp., and Pseudomonas fluorescens under dynamic flow conditions. PLoS One 2012;7:1–8. https://doi.org/ 10.1371/journal.pone.0050560.
- [14] Wong V, Levi K, Baddal B, Turton J, Boswell TC. Spread of *Pseudomonas fluorescens* due to contaminated drinking water in a bone marrow transplant unit. J Clin Microbiol 2011;49:2093–6. https://doi.org/10.1128/JCM.02559-10.
- [15] Donlan R, Murga R, Carpenter J, Brown E, Besser R, Fields B. Monochloramine disinfection of biofilm-associated Legionella pneumophila in a potable water model system. In: Marre R, Kwaik YA, Bartett C, Cianciotto NP, Fields S, Frosch M, Hacker J, Luck PC, editors. Legionella. American Society for Microbiology; 2001. p. 406–10.
- [16] Gomes IB, Meireles A, Gonçalves AL, Goeres DM, Sjollema J, Simões LC, Simões M. Standardized reactors for the study of medical biofilms: a review of the principles and latest modifications. Crit Rev Biotechnol 2018;38:657–70. https://doi.org/10.1080/07388551.2017.1380601.
- [17] Keevil CW. Continuous culture models to study pathogens in biofilms. Methods Enzymol 2001;337:104–22. https://doi.org/10.1016/S0076-6879(01)37010-6.
- [18] Narciso DAC, Pereira A, Dias NO, Monteiro M, Melo LF, Martins FG. 3D optical coherence tomography image processing in BISCAP: characterization of biofilm structure and properties. Bioinformatics 2024;40:btae041. https://doi.org/ 10.1093/bioinformatics/btae041.
- [19] Narciso DAC, Pereira A, Dias NO, Melo LF, Martins FG. Characterization of biofilm structure and properties via processing of 2D optical coherence tomography images in BISCAP. Bioinformatics btac002 2022. https://doi.org/10.1093/bioinformatics/ btac002
- [20] Wilks SA, Keevil CW. Targeting species-specific low-affinity 16S rRNA binding sites by using peptide nucleic acids for detection of legionellae in biofilms. Appl Environ Microbiol 2006;72:5453–62. https://doi.org/10.1128/AEM.02918-05.
- [21] Xiao R, Kisaalita WS. Purification of pyoverdines of *Pseudomonas fluorescens* 2-79 by copper-chelate chromatography. Appl Environ Microbiol 1995;61:3769–74. https://doi.org/10.1128/aem.61.11.3769-3774.1995.

- [22] Manuel CM, Nunes OC, Melo LF. Unsteady state flow and stagnation in distribution systems affect the biological stability of drinking water. Biofouling 2010;26: 129–39. https://doi.org/10.1080/08927010903383448.
- [23] Mauchline WS, Araujo R, Wait R, Dowsett AB, Dennis PJ, Keevil CW. Physiology and morphology of *Legionella pneumophila* in continuous culture at low oxygen concentration. Microbiology 1992;138:2371–80. https://doi.org/10.1099/ 00221287-138-11-2371.
- [24] Gloag ES, Wozniak DJ, Wolf KL, Masters JG, Daep CA, Stoodley P. Arginine induced Streptococcus gordonii biofilm detachment using a novel rotating-disc rheometry method. Front Cell Infect Microbiol 2021;11. https://doi.org/10.3389/ fcimb.2021.784388.
- [25] Paul E, Ochoa JC, Pechaud Y, Liu Y, Liné A. Effect of shear stress and growth conditions on detachment and physical properties of biofilms. Water Res 2012;46: 5499–508. https://doi.org/10.1016/j.watres.2012.07.029.
- [26] Rochex A, Godon J-J, Bernet N, Escudié R. Role of shear stress on composition, diversity and dynamics of biofilm bacterial communities. Water Res 2008;42: 4915–22. https://doi.org/10.1016/j.watres.2008.09.015.
- [27] Walter M, Safari A, Ivankovic A, Casey E. Detachment characteristics of a mixed culture biofilm using particle size analysis. Chem Eng J 2013;228:1140–7. https://doi.org/10.1016/j.cei.2013.05.071.
- [28] Silva AR, Narciso DAC, Gomes LC, Martins FG, Melo LF, Pereira A. Proof-of-concept approach to assess the impact of thermal disinfection on biofilm structure in hot water networks. J Water Process Eng 2023;53:103595. https://doi.org/10.1016/j.jwpe.2023.103595.
- [29] Mikaty G, Soyer M, Mairey E, Henry N, Dyer D, Forest KT, Morand P, Guadagnini S, Prévost MC, Nassif X, Duménil G. Extracellular bacterial pathogen induces host cell surface reorganization to resist shear stress. PLoS Pathog 2009;5:e1000314. https://doi.org/10.1371/journal.ppat.1000314.
- [30] Aggarwal S, Poppele EH, Hozalski RM. Development and testing of a novel microcantilever technique for measuring the cohesive strength of intact biofilms. Biotechnol Bioeng 2010;105:924–34. https://doi.org/10.1002/bit.22605.
- [31] Hou J, Veeregowda DH, van de Belt-Gritter B, Busscher HJ, van der Mei HC. Extracellular polymeric matrix production and relaxation under fluid shear and mechanical pressure in *Staphylococcus aureus* biofilms. Appl Environ Microbiol 2017;84:e01516. https://doi.org/10.1128/AEM.01516-17. 17.
- [32] Rice KC, Davis KAT. Brief communication: confocal microscopy of oral streptococcal biofilms grown in simulated microgravity using a random positioning machine. Npj. Microgravity 2024;10:89. https://doi.org/10.1038/s41526-024-00427-y
- [33] Meegoda CS, Waak MB, Hozalski RM, Kim T, Hallé C. The benefits of flushing for mitigating legionella spp. in non-chlorinated building plumbing systems. Front Water 2023;5. https://doi.org/10.3389/frwa.2023.1114795.
- [34] Buckner E, Buckingham-Meyer K, Miller LA, Parker AE, Jones CJ, Goeres DM. Coupon position does not affect Pseudomonas aeruginosa and Staphylococcus aureus biofilm densities in the CDC biofilm reactor. J Microbiol Methods 2024;223: 106960. https://doi.org/10.1016/j.mimet.2024.106960.
- [35] An S-Q, Hull R, Metris A, Barrett P, Webb JS, Stoodley P. An in vitro biofilm model system to facilitate study of microbial communities of the human oral cavity. Lett Appl Microbiol 2022;74:302–10. https://doi.org/10.1111/lam.13618.
- [36] Carine D, Coralie G, Mérilie G, Denis R, Julie J. Biofilm formation by heat-resistant dairy bacteria: multispecies biofilm model under static and dynamic conditions. Appl Environ Microbiol 2023;89:e00713. https://doi.org/10.1128/aem.00713-23.
- [37] Pant K, Palmer J, Flint S. Evaluation of single and multispecies biofilm formed in the static and continuous systems. Int J Food Microbiol 2025;429:111030. https://doi.org/10.1016/j.iifoodmicro.2024.111030.
- [38] Armbruster CR, Forster TS, Donlan RM, O'Connell HA, Shams AM, Williams MM. A biofilm model developed to investigate survival and disinfection of Mycobacterium mucogenicum in potable water. Biofouling 2012;28:1129–39. https://doi.org/10.1080/08927014.2012.735231.
- [39] Silva AR, Keevil CW, Pereira A. Legionella pneumophila response to shifts in biofilm structure mediated by hydrodynamics. Biofilm 2025;9:100258. https://doi.org/ 10.1016/j.biofim.2025.100258.
- [40] Flemming HC, Wingender J, Szewzyk U, Steinberg P, Rice SA, Kjelleberg S. Biofilms: an emergent form of bacterial life. Nat Rev Microbiol 2016;14:563–75. https://doi.org/10.1038/nrmicro.2016.94.

- [41] Walker JT, Mackerness CW, Rogers J, Keevil CW. Heterogeneous mosaic biofilm a haven for waterborne pathogens. In: Lappin-Scott HM, Costerton JW, editors. Microbial biofilms. Cambridge: Cambridge University Press; 1995. p. 196–204.
- [42] Grimard-Conea M, Prévost M. Controlling Legionella pneumophila in showerheads: combination of remedial intervention and preventative flushing. Microorganisms 2023;11:1361. https://doi.org/10.3390/microorganisms11061361.
- [43] Allerón L, Khemiri A, Koubar M, Lacombe C, Coquet L, Cosette P, Jouenne T, Frere J. VBNC *Legionella pneumophila* cells are still able to produce virulence proteins. Water Res 2013;47:6606–17. https://doi.org/10.1016/j.watres.2013.08.032.
- [44] Alleron L, Merlet N, Lacombe C, Frère J. Long-term survival of Legionella pneumophila in the viable but nonculturable state after monochloramine treatment. Curr Microbiol 2008;57:497–502. https://doi.org/10.1007/s00284-008-9275-9.
- [45] Mustapha P, Epalle T, Allegra S, Girardot F, Garraud O, Riffard S. Monitoring of Legionella pneumophila viability after chlorine dioxide treatment using flow cytometry. Res Microbiol 2015;166:215–9. https://doi.org/10.1016/j. resmic.2015.01.004.
- [46] Xu R, Zhu X, Sheng K, Tang Y, Zhang Y. Study of chlorine disinfection on the formation and resuscitation of viable but nonculturable (VBNC) bacteria in drinking water distribution systems. J Water Process Eng 2024;67:106216. https:// doi.org/10.1016/j.jwpe.2024.106216.
- [47] Gião MS, Wilks SA, Azevedo NF, Vieira MJ, Keevil CW. Validation of SYTO 9/ propidium iodide uptake for rapid detection of viable but noncultivable Legionella pneumophila. Microb Ecol 2009;58:56–62. https://doi.org/10.1007/s00248-008-0472.x
- [48] Farhat M, Trouilhé MC, Briand E, Moletta-Denat M, Robine E, Frère J. Development of a pilot-scale 1 for legionella elimination in biofilm in hot water network: heat shock treatment evaluation. J Appl Microbiol 2010;108:1073–82. https://doi.org/10.1111/j.1365-2672.2009.04541.x.
- [49] Dietersdorfer E, Kirschner A, Schrammel B, Ohradanova-Repic A, Stockinger H, Sommer R, Walochnik J, Cervero-Aragó S. Starved viable but non-culturable (VBNC) legionella strains can infect and replicate in Amoebae and human macrophages. Water Res 2018;141:428–38. https://doi.org/10.1016/j. watres.2018.01.058.
- [50] Buse HY, Lu J, Struewing IT, Ashbolt NJ. Eukaryotic diversity in premise drinking water using 18S rDNA sequencing: implications for health risks. Environ Sci Pollut Res 2013;20:6351–66. https://doi.org/10.1007/s11356-013-1646-5.
- [51] Gião MS, Wilks SA, Keevil CW. Influence of copper surfaces on biofilm formation by Legionella pneumophila in potable water. Biometals 2015;28:329–39. https://doi. org/10.1007/s10534-015-9835-y.
- [52] Rhoads WJ, Sindelar M, Margot C, Graf N, Hammes F. Variable legionella response to building occupancy patterns and precautionary flushing. Microorganisms 2022; 10:555. https://doi.org/10.3390/microorganisms10030555.
- [53] Gavaldà L, Garcia-Nuñez M, Quero S, Gutierrez-Milla C, Sabrià M. Role of hot water temperature and water system use on legionella control in a tertiary hospital: an 8-year longitudinal study. Water Res 2019;149:460–6. https://doi.org/ 10.1016/j.watres.2018.11.032.
- [54] Völker S, Schreiber C, Kistemann T. Modelling characteristics to predict legionella contamination risk - surveillance of drinking water plumbing systems and identification of risk areas. Int J Hyg Environ Health 2016;219:101–9. https://doi. org/10.1016/j.iijheb.2015.09.007.
- [55] Pereira A, Silva AR, Melo LF. Legionella and Biofilms—Integrated surveillance to bridge science and real-field demands. Microorganisms 2021;9:1212. https://doi. org/10.3390/microorganisms9061212.
- [56] Pereira A, Melo LF. Online biofilm monitoring is missing in technical systems: how to build stronger case-studies? npj Clean Water 2023;6:36. https://doi.org/ 10.1038/s41545-023-00249-7.
- [57] Nisar MA, Ross KE, Brown MH, Bentham R, Best G, Whiley H. Detection and quantification of viable but non-culturable *Legionella pneumophila* from water samples using flow cytometry-cell sorting and quantitative PCR. Front Microbiol 2023;14. https://doi.org/10.3389/fmicb.2023;1094877.
- [58] Grimard-Conea M, Deshommes E, Doré E, Prévost M. Impact of recommissioning flushing on Legionella pneumophila in a large building during the COVID-19 pandemic. Front Water 2022;4. https://doi.org/10.3389/frwa.2022.959689.
- [59] Cavallaro A, Gabrielli M, Hammes F, Rhoads WJ. The impact of DNA extraction on the quantification of *legionella*, with implications for ecological studies. Microbiol Spectr 2024;12:e00713. https://doi.org/10.1128/spectrum.00713-24. 24.